

Correlation waves after quantum quenches in one- to three-dimensional BECs

P. Deuar¹ and M. Stobińska^{2,1}

¹*Institute of Physics, Polish Academy of Sciences, Al. Lotników 32/46, 02-668 Warsaw, Poland*

²*Institute for Theoretical Physics and Astrophysics, University of Gdańsk, Gdańsk, Poland*

(Dated: August 30, 2018)

We obtain the universal form of spatial density and phase correlations after a quantum quench in dilute ultracold Bose gases, and give compact time-dependent expressions for the most visible effects. A Bogoliubov description in a local density approximation is used. It is demonstrated that density correlations can be observed even with imaging resolution well below healing length, and estimated that the conditions in existing 1D experiments allow observation of the long-range density correlation wave. This would allow one to directly measure counterpropagating atom pairs *in situ*.

Cold atom systems have enabled the investigation of non-equilibrium quantum dynamics to an unprecedented degree [1]. They allow one to prepare a known eigenstate of the system, precisely control its time-dependent Hamiltonian, and study its real-time dynamics. Changes to the Hamiltonian that occur globally and non-adiabatically in such a system realize a quantum quench, one of the fundamental quantum dynamical phenomena in many-body systems and cosmology. In interacting systems, time-varying spatial correlations are induced, and indeed measured in recent cold atom experiments [2–5]. There, a quantum quench can be willfully imposed by varying the tight confinement, the interaction strength with Feshbach resonances, or coupling internal states with laser fields. It can also occur as a side effect: when preparing the initial state of reduced-dimensional gases, turning on an optical lattice, or from a rapid loss of atoms that affects the chemical potential. The way that equilibration of nearly integrable systems after a quench scales with system size is an important open problem in quantum statistical mechanics [6].

Recent work on correlations after quantum quenches of ultracold bosons has mostly focused on the strong interaction regimes: Optical lattice systems implementing a Bose-Hubbard model quenched through or near the Mott/superfluid transition [2, 3, 6–12], continuum one-dimensional (1D) systems quenched into the fermionized regime [13–18] or with hard-core bosons [19]. For more dilute gases, the comprehensive work of Calabrese, Caux, and Cardy on the dynamical structure factor after a quench is widely applicable [20–22], including for the Lieb-Liniger 1D model [23, 24], and its long-time steady state [25]. Density correlations and waves in a 3D BEC were studied by Carusotto *et al.* [26]. Density structure factors have also been measured recently in 2D dilute gases [4, 5].

In this Letter we describe the real-space behavior of dilute gases after a quench of the interaction strength g in all dimensionalities and for all post-quench times in the Bogoliubov approximation. This provides results

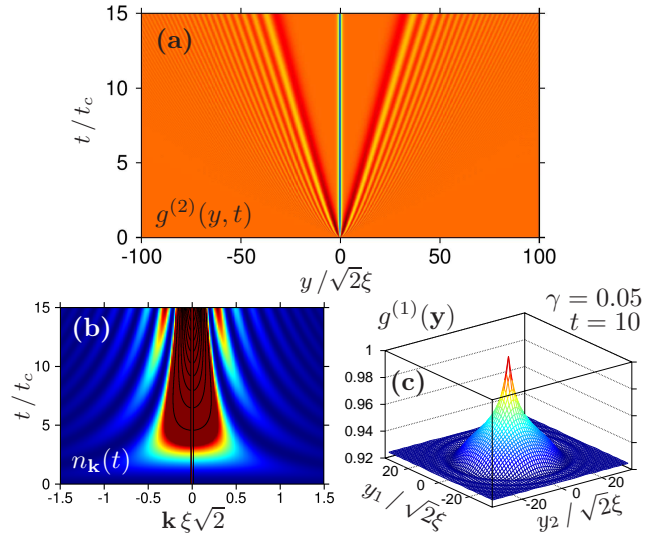


FIG. 1: Correlations after a quantum quench at $t = 0$ in dilute BECs: Density correlation $g^{(2)}(y, t)$ (a) and momentum distribution $n_{\mathbf{k}}(t)$ (b) in a 1D gas, and a snapshot of the phase correlation $g^{(1)}(\mathbf{y})$ in 2D. Red/blue values indicate high/low values, brown in (b) is a saturated high value, with black higher contours superposed. The healing length ξ , distance y , and time unit $t_c = \hbar/mc^2$ are as in the text.

for the whole gamut of phase and density correlation evolution in real space beyond the two earlier studies of particular cases [25, 26], and includes medium times in 1D, which we find to be especially favorable for observations. The first and second-order spatial correlation functions, $g^{(1)}$ and $g^{(2)}$, give an intuitive picture of the behavior that occurs in single realizations of the gas, something that is not usually directly accessible. They are found to have a universal form and evolution with a scale governed by the healing length in the gas. Examples are shown in Fig. 1. The shape of the correlations matches the shape of typical disturbances in the gas. We will describe the conditions to observe them in existing experiments with imperfect detection resolution. Our results also apply to quenches of the Bose-Hubbard model in the superfluid regime.

We will study the case of uniform gases with peri-

odic boundary conditions. Under typical experimental conditions the length scale of the correlations is sufficiently small that a local density approximation can be applied [27] to cover all short- and medium-scale phenomena. Experiments close to true uniform models have also been demonstrated, e.g. in a ring trap [28].

A d -dimensional Bose gas with s -wave contact interactions of strength g has the Hamiltonian

$$\hat{H} = \int d^d \mathbf{x} \hat{\Psi}^\dagger(\mathbf{x}) \left[-\frac{\hbar^2}{2m} \nabla^2 + \frac{g}{2} \hat{\Psi}^\dagger(\mathbf{x}) \hat{\Psi}(\mathbf{x}) \right] \hat{\Psi}(\mathbf{x}) \quad (1)$$

in terms of a Bose field $\hat{\Psi}(\mathbf{x})$, with mean density \bar{n} . It has just one dimensionless parameter which we will take as $\gamma = \frac{mg\bar{n}}{\hbar^2} d / \bar{n}^2$ which is $\ll 1$ in a dilute gas. It is self-same with the Lieb-Liniger gamma parameter in the 1D gas [29], and $\gamma = (4\pi)^3 \bar{n} a_s^3$ in 3D, in terms of the gas parameter $\bar{n} a_s^3 \ll 1$ and s -wave scattering length a_s . In reduced dimensionalities, the confinement in the tightly bound directions affects γ , e.g. with tight trapping frequency ν_\perp , $g = 4\pi \hbar a_s \nu_\perp$ in 1D. We now introduce dimensionless units: $\hbar = m = c = 1$, with $c = \sqrt{g\bar{n}/m}$ the speed of sound, and length and time units of $u_x = \hbar/mc$ and $t_c = mu_x^2/\hbar = \hbar/mc^2$, respectively. The BEC healing length (for all d) is then $\xi = 1/\sqrt{2}$, while $\gamma = 1/\bar{n}^2$.

Space of volume $V = L^d$ can be discretized on an arbitrarily fine lattice with volume Δv per point \mathbf{r}_i , giving a Bose-Hubbard Hamiltonian

$$\hat{H} = -J \sum_i \hat{a}_i^\dagger \hat{a}_{i+1} + \text{H.c.} + U \sum_i \hat{a}_i^\dagger \hat{a}_i^\dagger \hat{a}_i \hat{a}_i, \quad (2)$$

in terms of creation and annihilation \hat{a}_i operators on the lattice with $J = 1/[2(\Delta v)^{2/d}]$, $U = \sqrt{\gamma}/(2\Delta v)$, and mean site occupation $\Delta v/\sqrt{\gamma}$. Since a distance scale of at least the healing length is required to encompass the continuum physics, we need $\Delta v \ll 1$ for the mapping of the continuum onto a lattice to be sensible. On a square lattice, Δv corresponds to a maximum momentum cutoff $k_{\max} = \pi/(\Delta v)^{(1/d)}$, and so $J/U = (1/\sqrt{\gamma})(k_{\max}/\pi)^{2-d}$.

The system at $t < 0$ is taken to be the $\gamma = 0$ non-interacting uniform condensate of N atoms in the zero momentum ($\mathbf{k} = 0$) mode, with the interaction instantaneously turned on to its final value $\gamma > 0$ at $t = 0$.

The evolution is treated using a standard number-conserving Bogoliubov description [30], with similarities to [26]. The Bogoliubov approach boils down to two assumptions: (I) That quantum depletion $\delta N/N$, being the fraction of atoms in the non-condensate modes, is much smaller than one, and (II) that the interaction between non-condensate modes can be neglected. Such interactions are a higher order in the small parameter ($\delta N/N$) than the interaction between

the condensate and any of these modes. In a dilute gas with $\gamma \ll 1$, both assumptions are met. This corresponds to remaining deep in the superfluid regime ($J/U \gg 1$) of the Bose-Hubbard model.

We find the following: In terms of the dispersion relation for $k = |\mathbf{k}|$: $\omega_k = k\sqrt{1+k^2/4}$, the normalized phase coherence at a distance $y = |\mathbf{y}|$ between two points \mathbf{r} and $\mathbf{r}' = \mathbf{r} + \mathbf{y}$ is described by

$$g^{(1)}(y, t) = \langle \hat{a}^\dagger(\mathbf{r}) \hat{a}(\mathbf{r}') \rangle / (\bar{n} \Delta v) = 1 - \frac{1}{2\bar{n}V} \sum_{\mathbf{k} \neq 0} \frac{1}{\omega_k^2} \times [1 - \cos 2\omega_k t - \cos \mathbf{k} \cdot \mathbf{y} + \cos(\mathbf{k} \cdot \mathbf{y} + 2\omega_k t)]. \quad (3)$$

The normalized density correlations are

$$g^{(2)}(y, t) = \langle \hat{a}^\dagger(\mathbf{r}) \hat{a}^\dagger(\mathbf{r}') \hat{a}(\mathbf{r}') \hat{a}(\mathbf{r}) \rangle / (\bar{n} \Delta v)^2 = 1 - \frac{1}{2\bar{n}V} \sum_{\mathbf{k} \neq 0} \frac{k^2}{\omega_k^2} [\cos \mathbf{k} \cdot \mathbf{y} - \cos(\mathbf{k} \cdot \mathbf{y} + 2\omega_k t)]. \quad (4)$$

The mode occupation is $n_{\mathbf{k}} = [(\sin \omega_k t)/\omega_k]^2$, and quantum depletion $\delta N(t)/N = \frac{1}{N} \sum_{\mathbf{k} \neq 0} n_{\mathbf{k}}$. The correlations in momentum space are as expected for a Bogoliubov theory: $g^{(1)}(\mathbf{k}, \mathbf{k}') = \delta_{\mathbf{k}\mathbf{k}'}$, with Hanbury Brown-Twiss density fluctuations $g^{(2)}(\mathbf{k}, \mathbf{k}) = 2$ and pairing between counter-propagating momenta $g^{(2)}(\mathbf{k}, -\mathbf{k}) = 2 + 1/\bar{n}_{\mathbf{k}}$, with all other $g^{(2)}(\mathbf{k}, \mathbf{k}') = 1$.

In the large system and continuum limit $L \rightarrow \infty$, $\Delta v \rightarrow 0$, the discrete sums over \mathbf{k} can be converted to integrals. We find single universal solutions for each dimensionality d , as a function of t and distance y :

$$g^{(1)}(y, t) = 1 - \sqrt{\gamma} \int_0^\infty dk \left(\frac{1 - \cos 2\omega_k t}{k^2 + 4} \right) \frac{1 - M_d}{a_d k^{3-d}} \quad (5)$$

$$g^{(2)}(y, t) = 1 - \sqrt{\gamma} \int_0^\infty dk \left(\frac{1 - \cos 2\omega_k t}{k^2 + 4} \right) \frac{M_d k^{d-1}}{a_d}, \quad (6)$$

where the functions $M_d(ky)$ and constants a_d are

$$M_d = \begin{cases} \cos ky & \text{for } d = 1 \\ J_0[k|y|] & \text{for } d = 2 \\ \frac{\sin ky}{ky} & \text{for } d = 3 \end{cases}, \quad a_d = \begin{cases} \pi/2 & \text{for } d = 1 \\ \pi & \text{for } d = 2 \\ \pi^2 & \text{for } d = 3 \end{cases} \quad (7)$$

and $J_\alpha[x]$ are Bessel J functions. If the continuum assumption is relaxed, the only change is in the integration limits: $\int_0^{k_{\max}}$, which gives access to the Bose-Hubbard model. These are our main results, with interpretation to follow.

The deviation of correlations from full coherence $g^{(\mu)} = 1$ is proportional to $\sqrt{\gamma}$, and otherwise has a universal form. Several examples are shown in Fig. 1. Since the depletion must be small for Bogoliubov theory to apply, all expressions lose their validity if the correlations depart strongly from unity.

Simple expressions can be found from (5)-(6) in various limits. We present the medium- and long-time

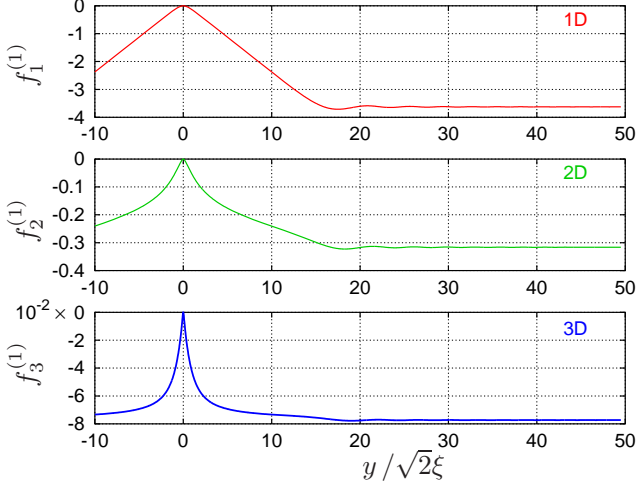


FIG. 2: Universal solutions (5) for phase coherence at long times $t = 7.5t_c$, shown scaled as $f_d^{(1)} = [g^{(1)}(y, t) - 1]/\sqrt{\gamma}$.

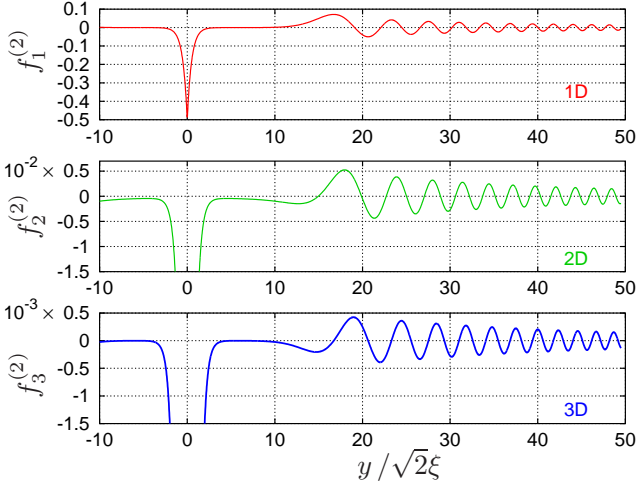


FIG. 3: Universal solutions (6) for density correlations at long times $t = 7.5t_c$, scaled as $f_d^{(2)} = [g^{(2)}(y, t) - 1]/\sqrt{\gamma}$.

correlations in the continuum limit below. Fig. 1(a), depicts the two principal regimes: a timelike regime inside the sound cone, and a spacelike one outside, with the main correlation wavepacket between them, propagating at twice the speed of sound. This speed arises because it is composed of atom pairs counterpropagating at $\geq c$. Representative snapshots of the correlations are shown in more detail in Figs. 2 and 3.

In the *spacelike regime* $y > 2t$, $t \gg 1$, the density fluctuations decay to $g_{\text{spacelike}}^{(2)} = 1$, while the reduction in phase coherence is equal to the depletion

$$g_{\text{spacelike}}^{(1)}(y, t) \approx 1 - \delta N(t)/N, \quad (8)$$

where at long times

$$\frac{\delta N(t)}{N} \approx \sqrt{\gamma} \times \begin{cases} \frac{4t-1}{8} & \text{for } d = 1 \\ \frac{1}{4\pi} \{c_1 + \log t\} & \text{for } d = 2 \\ \frac{1}{4\pi} (1 + c_2 e^{-c_3 t}) & \text{for } d = 3 \end{cases} \quad (9)$$

The main contributions to this reduction are from phonon excitations. The constants c_j are found numerically, and are $c_1 \approx 1.96(1)$, $c_2 \approx 0.43(1)$, and $c_3 \approx 2.24(2)$. We see the linear and logarithmic decay characteristic of 1D and 2D quasicondensates, respectively. In the 3D case, the loss of coherence stabilizes at a small constant value, as expected for a BEC. However, it is $\delta N/N = \frac{\sqrt{\gamma}}{4\pi} \approx 0.080\sqrt{\gamma}$ in the long time limit, which is less than the $T = 0$ equilibrium value of $\frac{2\sqrt{2\gamma}}{3\pi^2} \approx 0.096\sqrt{\gamma}$. This indicates that the quench does not initially access all the degrees of freedom available to the ground state, and resembles an effect that was recently found in the integrable 1D case [25]. That was attributed to initial state overlap conditions, which may also be a factor here as well as in 2D. Another symptom is that the momentum distribution, despite scaling with the expected fourth power: $n_{\mathbf{k}} \sim k^4$ when $k \gg 1$, contains the ‘‘holes’’ seen in Fig. 1(c). For lattices in 3D the depletion is particularly strongly dependent on the finite k_{max} , being $\delta N(t \rightarrow \infty)/N = \frac{\sqrt{\gamma}}{2\pi^2} \tan^{-1} \frac{k_{\text{max}}}{2}$ at long times.

In the *timelike regime* $y < 2t$, $t \gg 1$, the phase coherence decays for $y \gtrsim 1$ as

$$g_{\text{tl}}^{(1)}(y) \approx 1 - \sqrt{\gamma} \times \begin{cases} \frac{2y-1}{8} & \text{for } d = 1 \\ \frac{1}{4\pi} \{\gamma_E + \log y\} & \text{for } d = 2 \\ \frac{1}{4\pi} \left(1 - \frac{1}{2y}\right) & \text{for } d = 3 \end{cases} \quad (10)$$

to its spacelike value (8), with $\gamma_E \approx 0.5772$. Density correlations occur locally on the healing-length scale due to anti-bunching caused by inter-atomic repulsion:

$$g_{\text{tl}}^{(2)}(y) \approx 1 - \sqrt{\gamma} \times \begin{cases} \frac{e^{-2y}}{2} & \text{for } d = 1 \\ \frac{K_0[2y]}{\pi} & \text{for } d = 2 \\ \frac{e^{-2y}}{2\pi y} & \text{for } d = 3 \end{cases} \quad (11)$$

but are absent in the main body of the timelike regime. This is because no disturbance can travel slower than the speed of sound. $K_0[x]$ is the Bessel K function. For $d \geq 2$, the value at $y \ll 1$ bottoms out to a value determined rather by the lattice spacing, being $g^{(2)}(0) \approx 1 - \frac{\sqrt{\gamma}}{2\pi} \log(k_{\text{max}}^2/4)$ in 2D and $\approx 1 - \sqrt{\gamma}(k_{\text{max}}/\pi^2)$ in 3D when $k_{\text{max}} \gg 1$.

The main density correlation wave travels on the boundary between the spacelike and timelike regimes at $y \approx 2t$, and takes the forms:

$$g_{\text{wave}}^{(2)}(y) \approx 1 + \sqrt{\gamma} \times \begin{cases} \frac{1}{2(6t)^{1/3}} \text{Ai}[-x] & \text{for } d = 1 \\ \frac{1}{2\sqrt{\pi y} (6t)^{1/2}} F_2[-x] & \text{for } d = 2 \\ \frac{1}{2\pi y (6t)^{2/3}} F_3[-x] & \text{for } d = 3 \end{cases} \quad (12)$$

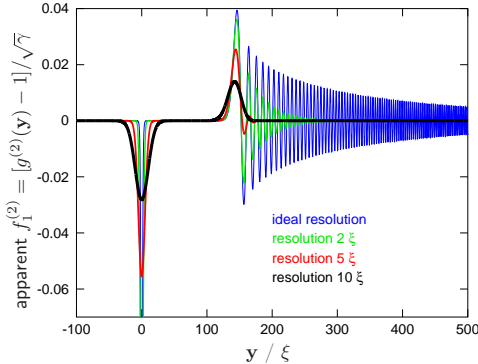


FIG. 4: Density correlations $g^{(2)}(\mathbf{y})$ at $t = 50t_c$ in 1D when seen with limited resolution.+

where $x = (\frac{4}{3t})^{1/3} [y - 2t]$ is a scaled coordinate measuring the distance to the sound cone edge, and Ai is the Airy function. The F_d functions are its generalizations

$$F_d[x] = \frac{1}{\pi} \int_0^\infty du u^{\frac{d-1}{2}} \cos \left[xu + \frac{u^3}{3} + \frac{\pi}{4}(d-1) \right] \quad (13)$$

such that $F_1[x] = \text{Ai}[x]$. There is also a less marked oscillation in the phase coherence $g^{(1)}$ at the same distances, on top of the dominant kink at the sound cone edge (see Fig. 2).

Current experiments, whether with absorption or phase-contrast imaging [31], have resolutions of many healing lengths ξ . Hence, the decay of coherence, $g^{(1)}$, inside the sound cone is directly resolvable, but not the antibunching dip or early correlation waves in $g^{(2)}$ (which must be measured *in situ*). However, the correlation wave retains its structure in the *scaled* length variable x , becoming magnified with time as $t^{1/3}$ and resolvable if the wave can survive intact for long enough. Simultaneously, from (12), its amplitude decays as $t^{(1+d)/6}$. In Fig. 4 we emulate imperfect resolution measurements by convolving long-time $g^{(2)}(y)$ with Gaussian point-spread functions of several widths. One sees that the primary correlation wave and the antibunching dip are robust to loss of resolution, remaining strongly visible and only mildly reduced in strength even with a (typical) resolution of 10ξ . The high-velocity component is rapidly lost. This resembles the distinct compact correlation wave seen with parity measurements in optical lattices [2].

To observe these waves in a simple manner, we should have (A) a gas that is long enough for the correlation wave to not meet the edge until it has broadened to a resolvable width, and (B) average over sufficiently many realizations for the correlation amplitude to emerge from the noise. Let us consider the conditions in some recent 1D gas experiments with ^{87}Rb in Vienna [31] ($N \approx 900$ to 11000 atoms, trap frequencies $\nu_x \times \nu_\perp \times \nu_\perp = 7 \times 1400 \times 1400$ Hz, imaging resolution

$3.8\mu\text{m}$) and Palaiseau ($N \approx 1200$ atoms, resolution $4.5\mu\text{m}$, trap frequencies $4 \times 3900 \times 3900$ Hz [27] and $7.5 \times 18800 \times 18800$ [32]). Consider the correlations induced by the quench in the center of the cloud and allow them to propagate half-way across, a distance y of one Thomas-Fermi radius. For the lower atom number in the Vienna experiment, the time is found to be $t \approx 28t_c$ (16ms), the rms width of the main peak rising above $g^{(2)} = 1$ is $w_{\text{rms}} = 1.802 \times t^{1/3}$, i.e. $3.5\mu\text{m}$, and the maximum height is $h_{\text{peak}} = 0.1474 \times \sqrt{\gamma}/t^{1/3}$, i.e. 0.004. The experimental resolution is in fact sufficient to resolve the structure even without the additional broadening seen in Fig. 4. For the correlation peak to rise out of the shot noise, one needs the statistical uncertainty to be less than h_{peak} . Taking a counting bin of the same size w_{rms} as the peak, with mean occupation $\overline{N}_{\text{bin}}$, and shot noise $\text{var}[N_{\text{bin}}] = \overline{N}_{\text{bin}}$, the variance of $g^{(2)}$ from one measurement is about $4\text{var}[N_{\text{bin}}]/\overline{N}_{\text{bin}}^2$. Hence, the minimum number of realizations to average over is $4/(\overline{N}_{\text{bin}}h_{\text{peak}}^2) \approx 4000$. Clouds with higher atom numbers are generally less favorable both with regard to width in μm which scales as $(N\nu_\perp\nu^4)^{-1/9}$, and the needed number of realizations, which scale as $(N^5\nu^2/\nu_\perp^4)^{1/9}$.

The first Palaiseau experiment [27] has comparable, slightly easier conditions, with propagation time $t \approx 80t_c$ (28ms), peak width $w_{\text{rms}} = 3.9\mu\text{m}$, max. height $h_{\text{peak}} \approx 0.006$, and 2500 required realizations. A comparison with the second experiment with tighter transverse confinement [32] and higher $\gamma \approx 0.17$ is instructive: $t \approx 190t_c$ (15ms), peak width $w_{\text{rms}} \approx 2.5\mu\text{m}$, max. height $h_{\text{peak}} = 0.011$, and 1400 required realizations. i.e. better signal to noise but a narrower wave (which will be alleviated by the spreading of Fig. 4). The waves may also become more visible at the edges of the cloud where γ is larger [27] and $\xi \propto 1/\sqrt{\overline{n}}$ wider.

To observe the disturbance, it is crucial that the highest amplitude part of the wave is mostly positive. In 2D and 3D, the strong dip seen in Fig. 3 and [26] cancels the majority of the leading peak's contribution when averaged. From (11), the integrated volume of $g^{(2)}$ displaced by the quench is $\frac{1}{2}\sqrt{\gamma}$, which is conserved during late-time evolution. This implies a decay of the averaged peak height like $t^{(2/3)-d}$.

In summary, we have found expressions for the universal form of spatial density and phase correlations after a quantum quench in dilute Bose gases (5-7), displayed in Figs. 2-3. The medium and long-time behavior is given as simple expressions (8-12) that are easily applied to assess what can be seen in a given experiment. Fig. 4 shows that these correlations can be observed even with presently available imaging resolution, and the conditions for this in recent 1D experiments [27, 31, 32] look realistic. Previously, counter-

propagating atom pairs were observed with momentum measurements after expansion such as [33–35]. Looking instead at spatial correlations allow one to actually directly observe counterpropagating atom pairs *in situ*.

We are grateful to Pasquale Calabrese, Peter Drummond, Tomasz Świsłocki, Thomas Gasenzer, Jan Zill, and Miłosz Panfil for helpful discussions. This research was supported by the Marie Curie European Reintegration Grant PERG06-GA-2009-256291 and by the Polish Government project 1697/7PRUE/2010/7.

-
- [1] A. Polkovnikov *et al.*, Rev. Mod. Phys. **83**, 863 (2011).
 [2] M. Cheneau *et al.*, Nature **481**, 484 (2012).
 [3] S. Trotzky *et al.*, Nature Physics **8**, 325 (2012).
 [4] C.-L. Hung, V. Gurarie, C. Chin, arXiv:1209.0011.
 [5] A. Rancon *et al.*, arXiv:1305.4594.
 [6] M. Rigol, Phys. Rev. Lett. **103**, 100403 (2009).
 [7] P. Barmettler *et al.*, Phys. Rev. A **85**, 053625 (2012).
 [8] C. Kollath, A. M. Lauchli, E. Altman, Phys. Rev. Lett. **98**, 180601 (2007).
 [9] M. Cramer *et al.*, Phys. Rev. Lett. **100**, 030602 (2008).
 [10] G. Roux, Phys. Rev. A **81**, 053604 (2010).
 [11] J.-S. Bernier *et al.*, Phys. Rev. A **85**, 033641 (2012).
 [12] M. Killi, S. Trotzky, A. Paramekanti, Phys. Rev. A **86**, 063632 (2012).
 [13] D. Muth, B. Schmidt, M. Fleischhauer, New J. Phys. **12**, 083065 (2010).
 [14] M. Kormos *et al.*, arXiv:1204.3889.
 [15] M. Kormos *et al.*, arXiv:1307.2142.
 [16] J. Mossel, J.-S. Caux, New J. Phys. **14**, 075006 (2012).
 [17] V. Gritsev, T. Rostunov, E. Demler, J. Stat. Mech. P05012, (2010).
 [18] J. Zill *et al.*, unpublished (2013).
 [19] M. Rigol, A. Muramatsu, M. Olshanii, Phys. Rev. A **74**, 053616 (2006).
 [20] P. Calabrese and J. Cardy, Phys. Rev. Lett. **96**, 136801 (2006).
 [21] P. Calabrese and J. Cardy, J. Stat. Mech. P06008, (2007).
 [22] P. Calabrese and J. Cardy, J. Stat. Mech. P10004, (2007).
 [23] J.-S. Caux, P. Calabrese and N. A. Slavnov, J. Stat. Mech. P01008, (2007).
 [24] J.-S. Caux, P. Calabrese, Phys. Rev. A **74**, 031605(R) (2006).
 [25] J. De Nardis *et al.*, arXiv:1308.4310.
 [26] I. Carusotto *et al.*, EPJD **56**, 391 (2010).
 [27] J. Armijo *et al.*, Phys. Rev. A **83**, 021605(R) (2011).
 [28] A. Ramanathan *et al.*, Phys. Rev. Lett. **106**, 130401 (2011).
 [29] E. H. Lieb and W. Liniger, Phys. Rev. **130**, 1605 (1963).
 [30] Y. Castin, R. Dum, Phys. Rev. A **57**, 3008 (1998).
 [31] M. Gring *et al.*, Science **337**, 1318 (2012).
 [32] T. Jacqmin *et al.*, Phys. Rev. Lett. **106**, 230405 (2011).
 [33] A. Perrin *et al.*, Phys. Rev. Lett. **99**, 150405 (2007).
 [34] R. G. Dall *et al.*, Phys. Rev. A **79**, 011601 (2009).
 [35] R. Bücker *et al.*, Nat. Phys. **7**, 608 (2011).